2005 International Symposium on Nonlinear
Theory and its Applications (NOLTA2005)
Bruges, Belgium, October 18-21, 2005

The Influence of Q-Control on the Non-linear Dynamics of Amplitude Modulation Atomic Force Microscopy

Ferdinand Jamitzky[†‡], Wolfram Bunk[†], Robert W. Stark[‡]

†Max-Planck-Institut f. Extraterrestrische Physik, Garching, Germany
‡ Center for Nanoscience, Ludwig-Maximilians-Universität, Theresienstr. 41, 80333 München, Germany
Email: fxj@mpe.mpg.de, whb@mpe.mpg.de, stark@nanomanipulation.de

Abstract– In tapping mode atomic force microscopy (AFM) the highly non-linear tip-sample interaction gives rise to complicated dynamics. Apart from the well known bi-stability under typical imaging conditions the system exhibits chaos-like dynamics at small average tip-sample distances, which are typical operation conditions for mechanical dynamic nano-manipulation. We have investigated the influence of Q-control on the non-linear behavior of the system. This was accomplished by numerically simulating the AFM tip modeled by a set of ordinary differential-difference equations. The time series data was analyzed employing non-linear analysis tools and spectral analysis. The information dimension was computed together with a bifurcation diagram and a Poincaré map and was compared to the Fourier Spectrogram.

1. Introduction

Since its invention in 1995 [1] the atomic force microscope (AFM) has become a widely used instrument for surface analysis with nanometer resolution. Various imaging modes including static and dynamic methods have been introduced. The most common techniques are contact mode - a quasi static mode - along with the dynamic measurement modes such as non-contact mode, tapping or intermittent contact mode, and ultrasonic mode.

For standard imaging under ambient conditions the amplitude modulation AFM is one of the most often used measurement modes [2, 3]. In this mode the amplitude of the oscillatory motion is used as a feedback signal to trace the surface topography. The quality factor of the force sensor determines the response time of the instrument.

The manipulation of the sensor response by an additional external feedback circuitry allows one to tune the response characteristics to purpose. This was demonstrated already in 1993 by Mertz and co-workers [4]. Such an external feedback circuitry that damps or un-damps the cantilever oscillations is referred to as Q-control. Current implementations of a Q-control rely on variable phase shifters [5-7], time delays [8] or on a direct control of the phase and an additional signal generator [9]. Practical applications of Q-control include an resolution enhancement on biological specimen [6, 10, 11] or the measurement of energy dissipation [7]. By reducing the Q-factor the response time of the amplitude signal can be decreased. This increases the bandwidth of a topography feedback in dynamic AFM [12]. The non-linear dynamics of an AFM that is operated with such a reduced (or increased) Q-factor will be investigated in the following.

2. Modeling

The cantilever is modeled as a multiple degree of freedom system (N=3) using the state space formalism as described in [13]. The Q-control was modeled as a pure time delay [14]. The non-linear boundary conditions at the tip-side are modeled as a non-linear output feedback. Such a feedback perspective on dynamic AFM [15, 16] allows for a numerically efficient investigation of the system dynamics [17].

The simulation was implemented using the non-linear DMT model for the tip-sample interaction [18] using Matlab 7 and Simulink. A model with N = 3 eigenmodes was employed. Material parameters were: E_t = 129 GPa; ν_t = 0.28, E_s = 70 GPa; ν_s = 0.3; H = 6.4 10^{-2} nm nN, γ = 0.031. The system was driven at the fundamental resonance ω_1. The driving amplitude was adjusted to a free response amplitude of A_0 = 20 nm. These are typical conditions for imaging in ambient conditions. The input and output coupling factors of an idealized rectangular beam with an idealized detection and a spring constant of k = 10 N/m were assumed. A quality factor of Q = 200 was assumed for all modes.

To model a dynamic force spectroscopy experiment as sketched in Fig. 1, the distance between the sample and the tip's rest position was reduced in logarithmic steps between z_s = 22 nm and z_s = 0.2 nm. After each step the system was allowed to equilibrate for at least 10 Q_{eff} cycles before data was extracted for further analysis by fast Fourier transformation (FFT) or other analysis tools.

3. Results and Discussion

Three different settings of the feedback parameter were investigated: (a) a negative value G = -0.01 (Q = 66), (b) the system without feedback (Q = 200), (c) a positive gain G = 0.0042 leading to Q = 800. The spectrograms (frequency vs. $\log_{10}(z_s)$) of the numerical dynamic force spectroscopy experiment are displayed in Fig. 2.

For the system with the enhanced q-factor (Q = 800) the system remained in the low-amplitude (attractive) regime during the approach. The fundamental prevails during the entire approach. Only shortly before the tip snaps to contact at z_s = 0.4 a weak sideband develops.

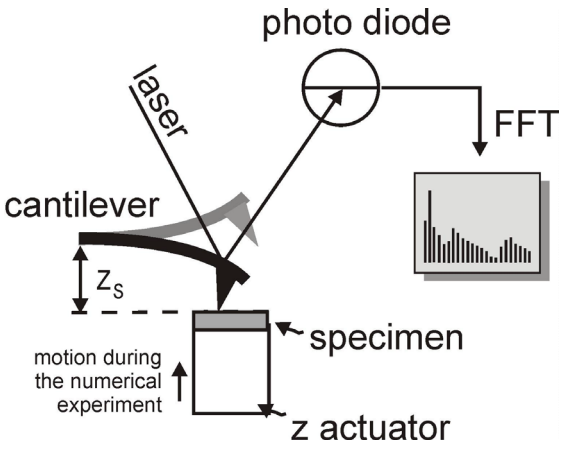

Fig. 1: Scheme of the dynamic force spectroscopy experiment as it was simulated numerically. The gap between the sample and the undeflected cantilever was reduced in logarithmic steps from $z_s = 22$ nm to $z_s = 0.2$ nm.

There was only a very slight harmonic distortion as it can be verified from the FFT spectrum. All harmonics are at least three orders of magnitude smaller as compared to the fundamental. In the case of the system without external feedback (Q = 200) there is a transition between the low amplitude and the high amplitude state at about 18 nm (Fig. 2b). In the transition regime sidebands with varying frequency can be identified. At about $z_s = 5$ nm period doubling occurs which is followed by a 1-periodic and an aperiodic regime.

For the system with Q = 66 the non-linear dynamics is even more pronounced. The system enters the repulsive regime immediately upon approaching the sample surface ($z_s \approx A_0$). During the first 10 nm of the approach the system remains periodic in the repulsive state. However, at $z_s = 9.048$ nm strong sidebands become visible (Fig. 2a). This frequency and amplitude of the sidebands varies slightly, until at $z_s = 4.928$ nm the system recovers to a 1-periodic behavior. This is followed by a period-doubling bifurcation with period-2 at $z_s = 3.882$ nm, period-4 at $z_s = 1.856$ nm and period-8 at $z_s = 1.739$ nm before a weakly aperiodic response is achieved. Nevertheless, it should be noted that the excitation frequency still dominates the system response in this regime. Other spectral components are still one or two orders of magnitude smaller as compared to the response at excitation frequency.

In order to investigate the non-linear features of the system the time series of the deflection data has been embedded into a three-dimensional phase space by using delay coordinates [19,20]. As delay times fractions of the natural system time scale have been used, namely: T/4 and T/8 where T is the period of the driving force. Three dimensional plots of the embedding are shown in Fig. 3 for the case Q=66 where the most pronounced non-linear behavior is found. The panels correspond to the period doubling, the period 4, period 8 and a weak chaotic regime respectively.

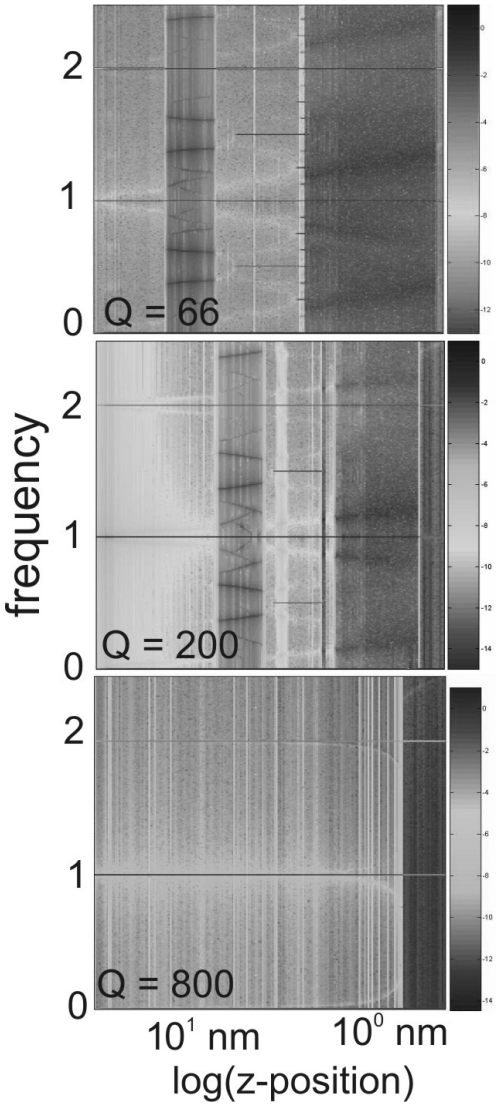

Fig. 2: Spectrograms as obtained for a reduced q-factor, the uncontrolled system and an enhanced q-factor. Note the logarithmic scale for the z-position z_s of the sample.

One can nicely observe how the initial trajectory splits into two sub-cycles (a) which then further split into additional cycles (b) until a whole torus in phase space is covered (d). Then a larger phase space volume is filled (e) until the system shows strong chaos. The non-linear behavior can be further characterized using a measure for the distribution of the trajectory in the phase space [21]. One such measure which is well suited for this purpose is the so called information dimension D1. It describes the scaling of the density of the trajectory points in phase space. A strongly periodic trajectory which is mapped to a circle in phase space has an information dimension of one. The more complicated the trajectory and thus the system behaves the larger the information dimension gets. For

strongly chaotic systems where the trajectory fills a part of the phase space densely the information dimension is close to two.

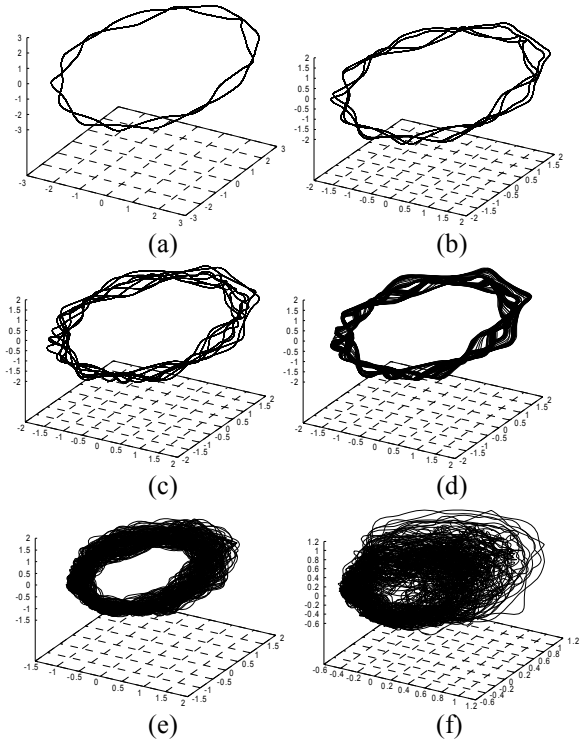

Fig. 3: Embeddings of the deflection data into a three-dimensional phase space by using a delay of T/8 and T/4 for different regimes: (a) period doubling regime (b) period 4 (c) period 8 (d) very large period (e) weak and (f) strong chaotic regime for Q=66.

In Fig. 4 the information dimension is shown for all three cases Q=66, 200 and 800 in dependence of the z-position of the tip. Far away from the surface D1 is close to one for all three cases. Under approaching the surface D1 is increasing strongly for Q=66 and Q=200 while it stays almost unity for Q=800. This means that the system Q=800 does not show chaotic signatures while the other two systems show a varying degree of chaoticity. In the case Q=66 the strongest chaotic behavior is observed which is reflected in a very early increase in the information dimension of the embedded trajectory. D1 increases as soon as the system shows a period doubling. This behavior is also observed in the Q=200 case, but here the period doubling starts later in the approach. The information dimension further shows regular windows where it decreases strongly which corresponds to a regular behavior of the system. The information dimensions corresponding to the different phase space plots in Fig.3 are: D1=1.04 for the period 2 case, D1=1.09 for the period 4 case, D1=1.125 for the period 8 case, D1=1.14 for the large period case, D1=1.28 and 1.79 for the weak and strong chaotic case. For the case (d) in Fig. 3 a Poincaré section has been computed which is shown in Fig. 5 (left). The lower right structure in the plot corresponds to the traversal into the plane, while the upper left structure corresponds to the traversal out of the plane. In the lower right structure there are four substructures visible which appear also in the upper left structure but in a different ordering. This reflects the stretch and fold mechanism in the attractor.

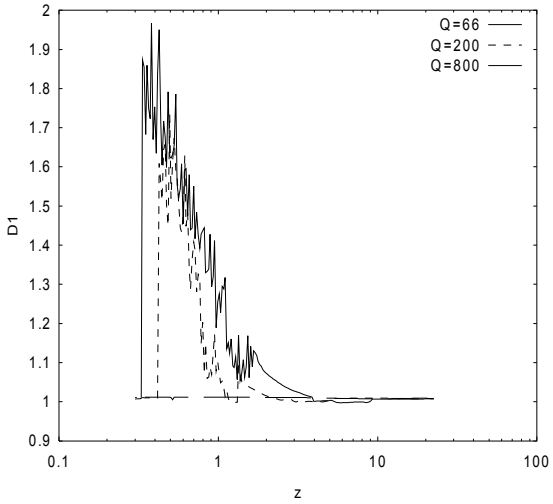

Fig. 4: Information Dimension D1 for all three cases Q=66, 200 and 800 vs. z-position of the tip. For the case Q=66 the largest dimension is obtained while for the case Q=800 the dimension stays at a value of 1 for the whole approach. The case Q=200 shows values larger than one but is overall smaller than Q=66.

By performing a stroboscopic view of the data one can draw a bifurcation diagram where the deflection amplitude is shown for a certain phase versus the tip-sample distance. In Fig.5 (right) such a bifurcation diagram is shown for Q=66. One can observe a period doubling in the system which after a cascade of further doublings leads into a chaotic state. There is a nice correlation of the bifurcation diagram with the plot of the information dimension. After the first period doubling the information dimension starts to rise from one to approx. 1.1 and then increases further to higher values, but decreases whenever the width of the black dots decreases in the bifurcation diagram. This can be explained by an increase of the chaoticity of the trajectories which leads to a higher information dimension and large variability in the bifurcation diagram. By comparing the bifurcation diagram with the spectrogram one can observe the period doubling cascade in both plots but the spectrogram does not show any substructure in the chaotic region while the bifurcation diagram and especially the information dimension plot shows different degrees of chaoticity. This is due to the lack of applicability of the Fourier transform to non-periodic signals. In these cases non-linear measures such as dimensions or entropies are the method of choice. For example in the case of weak chaos it is still possible to obtain reasonable information about the system by using Poincaré plots while the Fourier transform just shows a continuous spectrum.

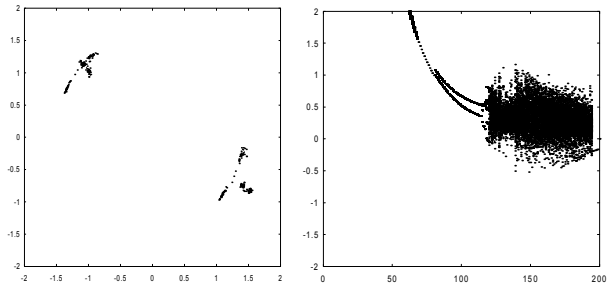

Fig. 5: (left) Poincaré section of the trajectory (d) in figure 3, (right) Bifurcation diagram for the system in the case Q=66.

4. Conclusions

The non-linear dynamic behavior of the system depends strongly on the Q value. For small Q values such as 66 or 200 a rich spectrum of irregular and chaotic motion is observed while for large Q values such as 800 the system behaves very regularly. For Q=66 a transition from regular behavior far away from the surface to chaotic behavior close to the surface has been found. A rich family of different types of trajectories can be observed where some of them show typical properties of chaotic systems such as a stretch and fold mechanism in phase space. The inherent chaoticity of the system can now be used in order to suppress the chaotic behavior and to stabilize the tip movement. One possibility would be the addition of noise to the signal to destruct the chaotic attractor and to confine the system to a regular behavior.

Acknowledgments

Financial support by the German Federal Ministry of Education and Research (BMBF, Grant 03N807) is gratefully acknowledged.

References

[1] G. Binnig, C. F. Quate, and C. Gerber, "Atomic Force Microscope," *Phys. Rev. Lett.*, vol. 56, pp. 930-933, 1986.

[2] R. García and R. Pérez, "Dynamic atomic force microscopy methods," *Surf. Sci. Rep.*, vol. 47, pp. 197-301, 2002.

[3] Q. Zhong, D. Inniss, K. Kjoller, and V. B. Elings, "Fractured polymer silica fiber surface studied by tapping-mode atomic-force microscopy," *Surf. Sci.*, vol. 290, pp. L688-L692, 1993.

[4] J. Mertz, O. Marti, and J. Mlynek, "Regulation of a microcantilever response by force feedback," *Appl. Phys. Lett.*, vol. 62, pp. 2344-2346, 1993.

[5] B. Anczykowski, J. P. Cleveland, D. Krueger, V. Elings, and H. Fuchs, "Analysis of the interaction mechanisms in dynamic mode SFM by means of experimental data and computer simulation," *Appl. Phys. A*, vol. 66, pp. S885-9, 1998.

[6] A. D. L. Humphris, A. N. Round, and M. J. Miles, "Enhanced imaging of DNA via active quality factor control," *Surface Science*, vol. 491, pp. 468-72, 2001.

[7] A. D. L. Humphris, J. Tamayo, and M. J. Miles, "Active quality factor control in liquids for force spectroscopy," *Langmuir*, vol. 16, pp. 7891-4, 2000.

[8] H. Hölscher, "Q-controlled dynamic force spectroscopy," *Surface Science*, vol. 515, pp. 517-22, 2002.

[9] J. Tamayo, M. Alvarez, and L. M. Lechuga, "Digital tuning of the quality factor of micromechanical resonant biological detectors," *Sensor Actuat B-Chem*, vol. 89, pp. 33-39, 2003.

[10] R. D. Jaggi, A. Franco-Obregon, P. Studerus, and K. Ensslin, "Detailed analysis of forces influencing lateral resolution for Q-control and tapping mode," *Appl. Phys. Lett.*, vol. 79, pp. 135-137, 2001.

[11] J. Tamayo, A. D. L. Humphris, R. J. Owen, and M. J. Miles, "High-Q dynamic force microscopy in liquid and its application to living cells," *Biophys. J.*, vol. 81, pp. 526-37, 2001.

[12] T. Sulchek, R. Hsieh, J. D. Adams, G. G. Yaralioglu, S. C. Minne, C. F. Quate, J. P. Cleveland, A. Atalar, and D. M. Adderton, "High-speed tapping mode imaging with active Q control for atomic force microscopy," *Appl. Phys. Lett.*, vol. 76, pp. 1473-1475, 2000.

[13] R. W. Stark, G. Schitter, M. Stark, R. Guckenberger, and A. Stemmer, "State-space model of freely vibrating and surface-coupled cantilever dynamics in atomic force microscopy," *Phys. Rev. B*, vol. 69, pp. 085412, 2004.

[14] R. W. Stark, "Force feedback in dynamic atomic force microscopy," presented at ASME IMECE, Orlando, Florida, 2005.

[15] A. Sebastian and M. V. Salapaka, "Analysis of periodic solutions in tapping-mode AFM: an IQC approach," presented at MTNS 02: 15th International Symposium on Mathematical Theory of Networks and Systems. 12 16 Aug. 2002 Notre Dame, IN, USA, 2002.

[16] M. Stark, R. W. Stark, W. M. Heckl, and R. Guckenberger, "Inverting dynamic force microscopy: From signals to time-resolved interaction forces," *Proc. Natl. Acad. Sci. USA*, vol. 99, pp. 8473-8478, 2002.

[17] R. W. Stark, "Spectroscopy of higher harmonics in dynamic atomic force microscopy," *Nanotechnology*, vol. 15, pp. 347-51, 2004.

[18] B. V. Derjaguin, V. M. Muller, and P. Toporov Yu, "Effect of contact deformations on the adhesion of particles," *J. Coll. Interf. Sci.*, vol. 53, pp. 314-26, 1975.

[19] F. Takens, “Detecting Strange Attractors in Turbulence”, Lecture Notes in Math. vol. 898, Springer, New York, 1981.

[20] T. Sauer, J. Yorke, and M. Casdagli, “Embedology”, J. Stat. Phys., vol. 65, p. 579, 1991.

[21] R. Hegger, H. Kantz, and T. Schreiber, “Practical implementation of nonlinear time series methods: The TISEAN package”, Chaos, vol. 9, 413 (1999)